Trehalose Favors a Cutinase Compact Intermediate Off-Folding Pathway

Eduardo P. Melo,*[,‡,§] LuYang Chen,[§] Joaquim M. S. Cabral,[§] Peter Fojan,[||] Steffen B. Petersen,[||] and Daniel E. Otzen[||]

Centro de Biomedicina Molecular e Estrutural, Universidade do Algarve, Campus de Gambelas, 8005-139 Faro, Portugal, Centro de Engenharia Biológica e Química, Instituto Superior Técnico, Av. Rovisco Pais, 1049-001 Lisboa, Portugal, and Department of Biotechnology, Aalborg University, Sohngaardsholmsvej 49, DK 900 Aalborg, Denmark

Received February 18, 2003; Revised Manuscript Received May 2, 2003

ABSTRACT: The folding of cutinase, an enzyme displaying lipolytic activity, has been studied in the presence of trehalose. Equilibrium unfolding data show that trehalose increases the free energy change between folded and unfolded states. Unfolding kinetics reveal the presence of an intermediate which is ca. 60% folded in terms of solvent exposure. Trehalose stabilizes this intermediate relative to the folded state. In contrast, the intermediate revealed by folding kinetics is more compact than the transition state, as shown by the positive slope observed at low denaturant concentration in the chevron plot, as well as the decrease in the observable rate constant for folding with the increase in trehalose concentration. This intermediate displays more than 50% of area buried from the solvent (relative to the native state) compared to around 40% for the transition state for folding and therefore appears to be off the folding pathway. Trehalose stabilizes and guanidine hydrochloride destabilizes this compact intermediate. Both unfolding and folding kinetics show that compact conformational states are stabilized by trehalose, in agreement with current models on the effect of compatible solutes. This effect occurs even for compact states that decelerate the folding as in the case of the intermediate revealed by folding kinetics.

Among the existing methods to increase protein stability, the addition of compatible solutes (low molecular weight solutes which accumulate intracellularly as a response to stress conditions such as high temperature and salinity) has been used for a long time. The principles and the mechanism to explain protein stabilization by low molecular weight solutes have been well documented in several papers (*1*, *2*). However, few have shown the effect of these solutes and salts on the folding pathway of proteins which can also provide insight into the stabilization mechanism. These solutes have been used also to induce partially structured states in the refolding process (*3*, *4*). The sugar trehalose (α-D-glucopyranosyl α-D-glucopyranoside) is one of the most prevalent compatible solutes in nature. It is a nonreducing disaccharide produced in cyanobacteria and bacteria under moderate stress and in yeast under severe stress (*5*). In addition, it plays a key role in the survival of some plants and insects in harsh environments (*6*). Trehalose is among the most chemically unreactive sugars, and its strong stability is a result of the very low energy of the glycoside oxygen bond joining the two hexose rings. It is of biotechnological importance due to its effectiveness in stabilizing membrane structure, pharmaceutical preparations, and even organs for transplantation (*6*), decreasing biological damage at low temperature and stabilizing protein structure during freezing, freeze-drying, and heating. Its role as a stress protectant, including the stabilization of proteins at high temperatures, has been ascribed to its ability to suppress the aggregation of denatured proteins (*7*).

Cutinase is an enzyme displaying lipolytic activity (EC 3.1.1.3.) with a molecular mass around 22.5 kDa and an isoelectric point of 7.6 (*8*). Cutinase unfolding induced by GdnHCl at pH 4.5 was previously studied by equilibrium assays using several spectroscopic techniques, and an intermediate "molten globule" in character was identified (*9*). Refolding/unfolding kinetics are an useful approach to detect and study intermediates. In this work, kinetic intermediates during cutinase refolding and unfolding were detected and characterized to see how similar they are to the equilibrium intermediate according to the observations made with other proteins (*10*). Focus on the effect of trehalose on the stability and nature of the intermediates was specifically addressed to have insight on the mechanism of protein stabilization by trehalose. A new intermediate off-folding pathway was detected by refolding kinetics, and it was shown that trehalose stabilizes this compact intermediate.

MATERIALS AND METHODS

Cutinase from *Fusarium solani* was cloned and expressed in *Escherichia coli* WK-6 strain, a kind gift from Corvas International N.V. (Gent, Belgium). The recombinant enzyme has 197 residues [molecular mass 22500 Da, p*I* 7.6 (*8*)] and was produced and purified to a lyophilized powder of >95% purity (w/w) using an osmotic shock to disrupt cells followed by an ammonium sulfate precipitation and two anionic exchanger chromatographic steps (DEAE-Sephacel and Q-Sepharose).

* Correspondence should be addressed to this author at the Instituto Superior Técnico. E-mail: emelo@ualg.pt. Fax: 351 218419062. Phone: 351 218419068.

[‡] Universidade do Algarve.

[§] Instituto Superior Técnico.

[||] Aalborg University.

10.1021/bi034267x CCC: $25.00 © 2003 American Chemical Society
Published on Web 05/23/2003

Guanidine hydrochloride (GdnHCl) was obtained from Gibco/BRL Life Technologies (ultrapure) and trehalose from Sigma (>98.5%). All salts were of analytical grade.

All experiments were performed in 50 mM acetate buffer, pH 4.5 at 25 °C.

Equilibrium Unfolding. Unfolding of cutinase was induced by GdnHCl and measured using excitation at 280 nm and integrating the corrected emission spectra between 300 and 420 nm on a Perkin-Elmer MPF3 fluorescence spectrophotometer. Upon cutinase unfolding a 3-fold increase on the quantum yield was observed because the single tryptophan residue is removed from the quenching effect of the disulfide bond between Cys 31 and Cys 109 (*9*, *11*). Slits were set at 6 nm, and cutinase concentration was 4 μM, giving an absorbance value at 280 nm of 0.043 ($\epsilon = 10853 \pm 484$ M^{-1} cm^{-1} at 280 nm). For each data point in the unfolding experiment, 0.45 mL of cutinase stock solution was diluted into 2.25 mL of some buffer solution containing the appropriate denaturant concentration. Trehalose was dissolved in both solutions for the assays in the presence of trehalose. Baseline emission was observed in the presence of high concentrations of trehalose and was subtracted from sample emission.

Stopped-Flow Kinetics. Kinetic experiments were carried out on an Applied Photophysics SX-18MV reaction analyzer (Applied Photophysics, Leatherhead, Surrey, U.K.). The protein solution and GdnHCl solution were mixed in a 1:10 ratio to give a final protein concentration of 4 μM (unless otherwise stated) and the desired denaturant concentration. Whenever trehalose was used, it was present in both solutions. Unfolding was induced by mixing cutinase in buffer with the appropriate GdnHCl solution, and refolding was induced by mixing unfolded cutinase in 2 M (for the kinetics in the absence and presence of 0.25 M trehalose) or 2.2 M GdnHCl (for the kinetics in the presence of 0.75 M trehalose) with the appropriate GdnHCl solution. Double-jump experiments were carried out with symmetric mixing, and cutinase was first unfolded in 1.6 M GdnHCl and then allowed to refold after different delay periods in 0.8 M GdnHCl. Refolding into 0.20 and 0.37 M GdnHCl at different trehalose concentrations (from 0.1 to 1.0 M trehalose) and burst phase analysis were carried out on a Hi-Tech SF-41 stopped-flow reaction analyzer (Hi-Tech Scientific, Salisbury, U.K.) in a 1:6 ratio to give a final cutinase concentration of 15 μM. Excitation was always at 280 nm, and emission was detected above 315 nm using a glass filter. Burst phase analysis was carried out in the stopped-flow, including the measurement of equilibrium fluorescence intensities such as the fluorescence intensity of the unfolded state under unfolded conditions and that of the folded state under folded conditions. Fluorescence intensity measurements depend on several instrumental parameters and the measurement of equilibrium and kinetic amplitudes in the same instrument avoids normalization.

Data Analysis. Equilibrium unfolding was fitted to a two-state process according to the equations:

$$FI = FI_F f_F + FI_U f_U \quad (1)$$

$$K_{U-F} = f_U/f_F \quad (2)$$

$$\Delta G^\circ_{U-F} = -RT \ln K_{U-F} \quad (3)$$

$$\Delta G^\circ_{U-F} = \Delta G^\circ_{U-F}{}^{water} - m_{U-F}[GdnHCl] \quad (4)$$

$$[GdnHCl]_{U-F}{}^{50\%} = \Delta G^\circ_{U-F}{}^{water}/m_{U-F} \quad (5)$$

where F and U are folded and unfolded cutinase, respectively, FI is the fluorescence intensity, f is the fraction of cutinase molecules with a given conformation, K is the equilibrium constant, ΔG° is the standard free energy, m is the linear dependence of ΔG° on GdnHCl concentration, and $[GdnHCl]_{U-F}{}^{50\%}$ is the GdnHCl concentration for $\Delta G^\circ = 0$. FI_F and FI_U were calculated directly from the pre- and posttransition regions according to a linear dependence.

Kinetic unfolding data were fitted to a three-state process to describe the downward curvature observed for the unfolding limb according to Scheme 1 (*12*).

In this scheme, I is a transient intermediate formed during the dead time of the experiment. Therefore, rapid equilibrium between F and I was assumed, and the following equations can be used:

$$k_u{}^{obs} = f_I k_u \quad (6)$$

$$K_I = f_I/f_F \quad (7)$$

Considering a linear dependency of log K_I and log k_u on GdnHCl concentration, the following relationship holds:

$$\log k_u{}^{obs} = \log\left[\frac{10^{\log k_u{}^{water} + m_u{}^{\ddagger}[GdnHCl]}}{1 + \frac{1}{10^{\log K_I{}^{water} + m_{I\text{-}F}[GdnHCl]}}}\right] \quad (8)$$

Kinetic refolding data were fitted to considering a transient intermediate off-folding pathway, as shown in Scheme 2. In this scheme, C is a transient intermediate formed during the dead time of the experiment. Therefore, rapid equilibrium between C and U and linear dependencies of log K_C and log k_f on GdnHCl concentration were assumed, and the following relationships hold:

$$K_C = f_C/f_U \quad (9)$$

$$k_f{}^{obs} = f_U k_f \quad (10)$$

$$\log k_f{}^{obs} = \log\left[\frac{10^{\log k_f{}^{water} + m_f{}^{\ddagger}[GdnHCl]}}{1 + 10^{\log K_C{}^{water} + m_{C-U}[GdnHCl]}}\right] \quad (11)$$

GdnHCl concentration in eq 11 was in some cases replaced by trehalose concentration. For these cases K_C, k_f, and m values were depicted by $K_C{}^{0M\ trehalose}$, $k_f{}^{0M\ trehalose}$, $m_{C-U}{}^{trehalose}$, and $m_f{}^{\ddagger trehalose}$.

Equations 8 and 11 were used to fit kinetics of unfolding and refolding, respectively, using the Levenberg−Marquardt algorithm included in the nonlinear least-squares fitting capability of the Origin software, version 6.1. Since the parameters $m_f{}^{\ddagger}$ and $k_f{}^{water}$ are not linked to m_{C-U} and $K_C{}^{water}$, values for $m_f{}^{\ddagger}$ and log $k_f{}^{water}$ were first determined by linear regression of the folding limb of the chevron plot below the "rollover" region. Then eq 11 was fitted to all of the data in the refolding limb using values of $m_f{}^{\ddagger}$ and log $k_f{}^{water}$

Scheme 1

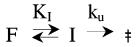

Scheme 2

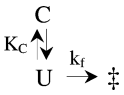

Table 1: Parameters for Unfolding of Cutinase at pH 4.5 in the Presence of Increasing Concentrations of Trehalose According to a Two-State Mechanism

	$\Delta G°_{U-F}{}^{water}$ (kcal/mol)	m_{U-F} (kcal mol^{-1} M^{-1})	$[GdnHCl]_{U-F}{}^{50\%}$ (M)
no trehalose	7.9 ± 0.2	6.7 ± 0.2	1.18 ± 0.07
0.25 M trehalose	9.7 ± 0.4	7.1 ± 0.3	1.37 ± 0.12
0.50 M trehalose	8.8 ± 0.3	5.6 ± 0.2	1.56 ± 0.11
0.75 M trehalose	9.8 ± 0.5	5.8 ± 0.3	1.70 ± 0.16
1 M trehalose	10.6 ± 0.4	5.6 ± 0.2	1.89 ± 0.14

previously determined to find the values of m_{C-U} and log $K_C{}^{water}$ which minimize the sum of squares of the deviations.

RESULTS

Equilibrium unfolding of cutinase induced by GdnHCl in the presence of different trehalose concentrations was studied by fluorescence intensity measurements (Figure 1). One stable intermediate at least is present at equilibrium as previously shown, based on noncoincident unfolding curves measured by near-UV absorbance, fluorescence intensity, and circular dichroism measurements (*9*). However, unfolding transitions were well fitted by a two-state mechanism because transitions from the folded to the intermediate and from this intermediate to the unfolded state are close, apparently giving a two-state mechanism. Therefore, the unfolding curves shown in Figure 1 were fitted to a two-state mechanism (F ↔ U) to a more accurate determination of the parameters which characterize the net transition from the folded to the unfolded state (Table 1). The stabilization of cutinase increases with trehalose concentration, as revealed by the increase in the midpoint. The free energy change in water tends also to increase despite some uncertainty due to the long extrapolation from the transition region. On the contrary, the *m* value tends to decrease, reflecting probably a more structured unfolded state in the presence of trehalose.

Refolding/unfolding kinetics are a powerful test for detecting intermediates. Unfolding of cutinase reveals only one phase, but folding shows clearly two phases (Figure 2). The amplitude of the slow phase for folding is 36 ± 3% of the total amplitude whether trehalose is present or not. The rate constant for the slow phase (between 0.046 and 0.015 s^{-1} for 0.18 and 1 M GdnHCl, respectively) is compatible with a *cis*−*trans* isomerization of peptidyl−prolyl bonds in solution, which has half-lives of 10−100 s (*12*). All of the peptidyl−prolyl bonds are *trans* for native cutinase (PDB entry 1AGY), but the *cis* isomer can be present in significant amounts for unfolded cutinase. Refolding from an aggregated state as observed for U1A (*13*) and chymotrypsin inhibitor 2 is excluded because kinetics are independent of cutinase concentration within the concentration range tested (1−4 μM) (data not shown). Double-jump experiments, in which cutinase was first unfolded and then allowed to refold after various periods of time, were performed to clarify the nature of the slow phase. The amplitude of the slow phase increases exponentially with the delay time with a rate constant of 0.022 ± 0.004 s^{-1} (half-life of 45 s) (Figure 3). This indicates that the denatured state equilibrates to a mixture of species with different refolding properties. Such equilibration is typical of a *cis*−*trans* isomerization (*14*). The amplitude and the rate constant of the slow phase were not affected significantly in the presence of trehalose.

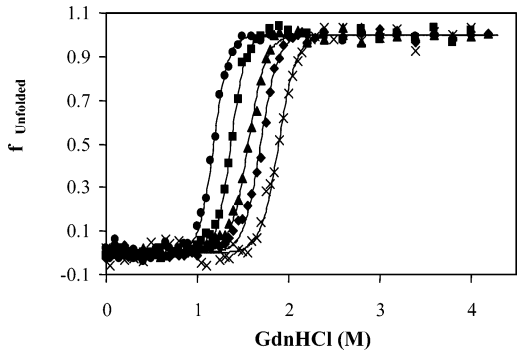

FIGURE 1: Unfolding of cutinase at pH 4.5 in the presence of increasing concentrations of trehalose: (●) no trehalose, (■) 0.25 M, (▲) 0.5 M, (◆) 0.75 M, and (×) 1 M trehalose. Solid lines fit unfolding curves according to the equation $f_U = e^{-\Delta G°/RT}/(1 + e^{-\Delta G°/RT})$.

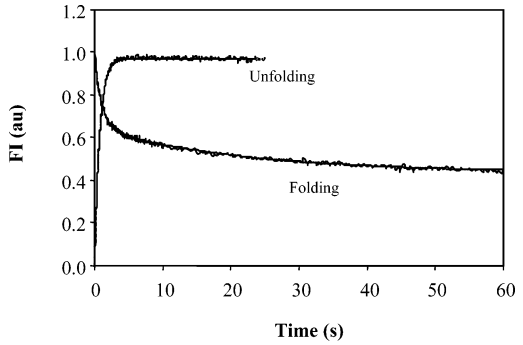

FIGURE 2: Time course for unfolding and refolding of cutinase at pH 4.5 followed by fluorescence intensity (excitation at 280 nm). Final GdnHCl concentrations were 2.0 and 0.18 M for unfolding and refolding, respectively. Solid lines are the exponential fittings analyzed on the Applied Photophysics software. Unfolding shows a single phase with rate constant of 1.309 s^{-1}, and refolding shows a slow phase and a fast phase with rate constants of 0.046 and 0.951 s^{-1}, respectively. The amplitudes were normalized considering the amplitude of unfolding as 1.

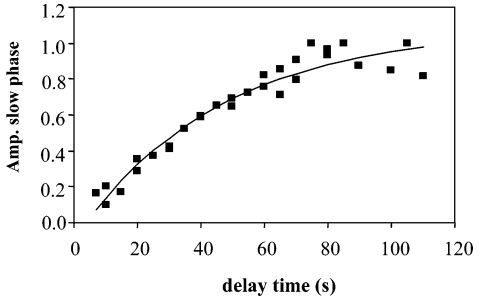

FIGURE 3: Change in the normalized amplitude of the slow phase of refolding with the delay time measured in a double-jump experiment. The solid line is a single exponential fit with a rate constant of 0.022 ± 0.004 s^{-1}.

Table 2: Kinetic Parameters for Unfolding and Refolding of Cutinase at pH 4.5 in the Presence of Increasing Concentrations of Trehalose According to Schemes 1 and 2, Respectively[a]

[trehalose] (M)	unfolding				refolding			
	$K_I^{water} \times 10^5$	m_{I-F} (M^{-1})	k_u^{water} (s^{-1})	$m^{\ddagger}_u$ (M^{-1} s^{-1})	K_C^{water}	m_{C-U} (M^{-1})	k_f^{water} (s^{-1})	$m^{\ddagger}_f$ (M^{-1} s^{-1})
0	3.0 ± 0.9	1.9 ± 0.0	2.7 ± 1.1	0.28 ± 0.06	8.7 ± 2.0	-3.9 ± 0.4	5.9 ± 1.0	-2.0 ± 0.1
0.25	2.0 ± 0.6	1.9 ± 0.1	1.6 ± 0.8	0.30 ± 0.06	13.0 ± 1.1	-2.5 ± 0.1	13.4 ± 3.0	-1.9 ± 0.1
0.50	0.8 ± 0.2	1.8 ± 0.0	4.4 ± 1.5	0.13 ± 0.04	nm[b]	nm	nm	nm
0.75	0.5 ± 0.1	1.8 ± 0.0	4.4 ± 1.2	0.08 ± 0.03	15.2 ± 0.9	-2.2 ± 0.1	9.5 ± 1.9	-1.3 ± 0.1

[a] See Materials and Methods. [b] nm = not measured.

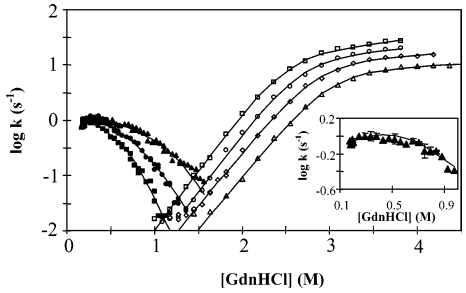

FIGURE 4: Chevron plot of the fast phase of refolding (solid symbols) and unfolding (open symbols) of cutinase. Unfolding data [(□) 0 M, (○) 0.25 M, (◇) 0.5 M, and (△) 0.75 M trehalose] conform to an unfolding intermediate accumulating during the dead time of the experiment as shown by the accuracy of the fit (solid lines are the fits using eq 8 for unfolding with an intermediate on-pathway). Refolding data [(■) 0 M, (●) 0.25 M, and (▲) 0.75 M trehalose] conform to a compact intermediate accumulating during the dead time of the experiment as shown by the accuracy of the fit (solid lines are the fits using eq 11 for refolding with an intermediate off-pathway). This intermediate displays less surface area exposed to the solvent than the transition state for folding as indicated by the positive slope identified at low GdnHCl concentration in the presence of 0.75 M trehalose (inset).

A chevron plot omitting the slow phase is shown in Figure 4. Two characteristics are evident: (i) the observable rate constants for refolding and unfolding do not meet at the transition region, confirming the presence of a stable intermediate within the transition region (this effect is more clearly observed with the increase on trehalose concentration), and (ii) the plot deviates from the simple V-shaped curve of log observed rate constant versus GdnHCl concentration on both refolding and unfolding limbs. This deviation has been ascribed to refolding and unfolding intermediates accumulating transiently at low and high GdnHCl concentrations, respectively, because of rollover pattern (*4*). Movements in the transition state position can also lead to curved chevron plots as observed for two small proteins (*15*, *16*). Distinction between the two hypotheses is difficult and can be based on the occurrence of a burst phase during kinetics (*17*) or on the dead-time spectra (*16*). If an intermediate accumulates in the dead time of the stopped-flow, the observable change in the kinetic amplitude will be different than expected because the spectroscopic properties of the intermediate are different from those of the initial state.

Figure 5 shows a burst phase analysis of the unfolding and refolding of cutinase. Unfolding shows no burst phase until 2.2 M GdnHCl (Figure 5A). Above this concentration the kinetic amplitudes show a small trend to be larger than expected. The unfolding limb of the chevron plot tends to a plateau precisely around this GdnHCl concentration, pointing to the accumulation of an intermediate. Apparently, it is difficult to rationalize the increase in the amplitude as resulting from an intermediate emitting less fluorescence than

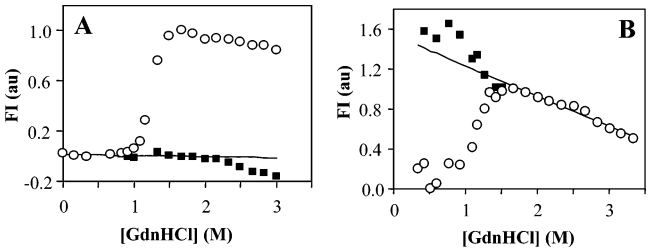

FIGURE 5: Kinetic and equilibrium amplitudes for the unfolding (A) and refolding (B) of cutinase at pH 4.5. Relative fluorescence (to a value of 1 for U) for the starting point of the kinetic curve obtained by extrapolation to $t = 0$ (■) and for the end point obtained by extrapolation to $t = \infty$ (○). The amplitudes of the two refolding phases were considered to extrapolate to $t = 0$. Solid lines are the fluorescence of the folded (A) and unfolded (B) states obtained by linear extrapolation.

the folded state since the unfolded state emits more fluorescence. As referred to above, the quantum yield of the folded state is very low (*11*) due to the quenching effect of a proximal disulfide bridge, and a decrease in the fluorescence intensity has to be caused by an intermediate with the tryptophan residue in a native environment. A movement in the transition state position cannot explain the unfolding pattern. A plateau is clearly observed, and the quadratic relationship used to quantify movements in the transition state (*15*, *16*) is unable to fit the plateau. Therefore, the rollover observed for the unfolding limb was described by considering the accumulation of an intermediate in the dead time of the experiment (Scheme 1), in line with the previous identification of an equilibrium intermediate (*9*) and the increase in the kinetic amplitude. Although an off-pathway intermediate cannot be formally excluded, an on-pathway mechanism provides a simpler and physically more plausible explanation of the rollover pattern (*10*). Increasing trehalose concentrations do not change the pattern in the unfolding limb, showing that the transient unfolding intermediate is still accumulating. The parameters obtained from the fits are shown in Table 2. Trehalose increases the free energy gap between folded and intermediate states (K_I^{water} decreases, leading to an increase in the free energy change from 6.2 to 7.2 kcal/mol for 0 and 0.75 M trehalose, respectively).

The refolding kinetic amplitude is larger than expected, pointing to the presence of an intermediate emitting more fluorescence than the unfolded state (Figure 5B). This observation is in line with the presence of a compact intermediate with no native contacts accumulating during the dead time of the refolding experiment according to Scheme 2 (see below). For an intermediate with non-native contacts, the tryptophan residue is not quenched by the disulfide bridge. At the same time the burying of the aromatic probes in the compact intermediate can increase its fluorescence emission as observed for several proteins (*16*, *17*).

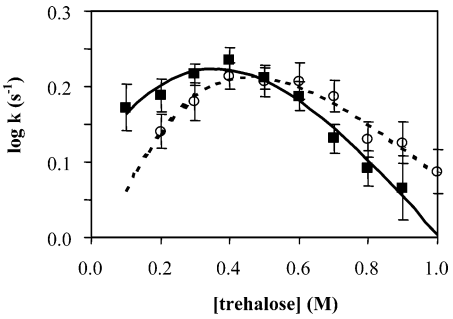

FIGURE 6: Refolding rate constants into 0.20 M (■) and 0.37 M (○) GdnHCl at different trehalose concentrations. The lines represent the best fit to eq 11 using trehalose concentration instead of GdnHCl concentration.

The presence of a compact intermediate during folding was evident in the presence of high trehalose concentrations. Trehalose changes the pattern in the refolding limb. Curves at different trehalose concentrations converge at low GdnHCl concentrations (Figure 4). Namely, in the presence of 0.75 M trehalose a positive dependence of the folding rate on GdnHCl concentration was observed at low denaturant concentration as shown clearly in the inset of Figure 4. This behavior was already observed at 0.25 M trehalose but only at 0.75 M was a positive slope clearly identifiable. The positive slope indicates that the transition state exposes more surface area than the kinetic ground state, and the data are consistent with an overcompact intermediate equilibrating with the unfolded state in the dead time of the experiment. The refolding limb of the chevron plot was fitted therefore according to Scheme 2 (parameters in Table 2). The overcompact intermediate C appears to be off the folding pathway. It is unlikely that an overcompact intermediate emitting more than the unfolded state (no native contacts) appears in a progressive folding scheme. Also, the sum of the kinetic *m* values approach the equilibrium *m* value if C is considered off-pathway. Increasing trehalose concentration stabilizes C relative to the unfolded state. The value of K_C^{water} (K_C = [C]/[U]) increases from 8.7 to 15.2 in the presence of 0.75 M trehalose, corresponding to an increase of 0.33 kcal/mol in the free energy change.

The stabilization of C by trehalose is even clearer when the refolding of cutinase is measured at increasing concentrations of trehalose and low GdnHCl concentration (Figure 6). Although its refolding rate initially increases as trehalose concentration increases, after a certain trehalose concentration a decrease in the rate was observed. In a progressive folding scheme with an intermediate on-pathway (U ↔ I ↔ N) it will be expected that the major transition state between I and N will be more stabilized by trehalose than the ground state less compact. This situation will lead to an increase in the refolding rate with increasing trehalose concentrations. The decrease observed in the refolding rate shows clearly the presence of an intermediate more compact than the major transition state for folding and therefore off-folding pathway (this intermediate will be more stabilized than the transition state). The decrease in the rate constant begins at high trehalose concentrations for high GdnHCl concentration. Trehalose and GdnHCl display opposite effects on the stability of C relative to the transition state for folding: Trehalose favors C and GdnHCl disfavors C. This effect was quantified by comparing K_C values. K_C^{water} in the absence of trehalose is 8.7 (Table 2) and decreases to 0.5 and 0.4 at 0.20 and 0.37 M GdnHCl concentration, respectively (Table 3). It is interesting to notice that an overcompact intermediate off the usual folding pathway was also observed for the two-state folding protein S6 from *Thermus thermophilus* in the presence of sodium sulfate although it may fold by an alternative pathway to the folded state (*3*).

Table 3: Effect of Trehalose and GdnHCl Concentration on the Stability of Compact Intermediate C (K_C) and the Refolding Parameters

[GdnHCl] (M)	$K_C^{0M\ trehalose}$	$m_{C-U}^{trehalose}$ (M^{-1})	$k_f^{0M\ trehalose}$ (s^{-1})	$m^{\ddagger}_{f}{}^{trehalose}$ ($M^{-1}\ s^{-1}$)
0.20	0.5 ± 0.3	1.8 ± 0.5	1.9 ± 0.3	1.3 ± 0.7
0.37	0.4 ± 0.1	2.2 ± 0.7	1.3 ± 0.2	1.9 ± 0.8

Table 4: Compactness of Intermediates and Transition States in Reference to Solvent Exposure Relative to That of the Folded State[a]

[trehalose] (M)	$\beta_f^{\ddagger}$ [b]	β_C [c]	β_I [d]	$\beta_u^{\ddagger}$ [e]
0	0.41	0.79	0.62	0.56
0.25	0.37	0.48	0.64	0.58
0.50	nm[f]	nm	0.56	0.53
0.75	0.31	0.51	0.58	0.56

[a] $\beta = 1$, folded state, and $\beta = 0$, unfolded state. [b] Calculated from $-2.303RTm^{\ddagger}_{f}/m_{U-F}$. [c] Calculated from $-2.303RTm_{C-U}/m_{U-F}$. [d] Calculated from $1 - (2.303RTm_{I-F}/m_{U-F})$. [e] Calculated from $1 - [2.303RT(m^{\ddagger}_{u} + m_{I-F})/m_{U-F}]$. [f] nm = not measured.

DISCUSSION

Characterization of folding/unfolding pathways of proteins in the presence of compatible solutes such as trehalose can provide some insight into the mechanism by which these solutes stabilize proteins. Intermediates and transition states in these pathways can be characterized by their β value (*12*). The parameter *m* is a constant related to the change in the solvent-accessible area between the initial and final state of the transition, and the ratio between *m* values (β value) is the fractional accessible area giving the average degree of exposure of intermediates or transition states relative to that of the folded state (Table 4). The unfolding kinetics at pH 4.5 suggest that an on-pathway intermediate I accumulates during the dead time of the experiment. This intermediate is around 60% folded in terms of solvent exposure ($\beta_I = 0.58-0.62$), and a stronger emission compared to the folded state will be expected since the quantum yield increases for the unfolded state. However, the intermediate emits less fluorescence than the folded state (Figure 5A), showing that the folded structure is maintained around the single tryptophan residue of cutinase. This kinetic intermediate shares characteristics with the equilibrium intermediate previously detected in the transition region (*9*). The equilibrium intermediate is 56% folded in terms of solvent exposure and emits almost the same fluorescence intensity as the folded state. Both equilibrium and kinetic intermediates were around 40% unfolded in terms of solvent exposure, but the tryptophan environment maintains its integrity. The transition state between I and U closely resembles I in terms of solvent exposure ($\beta_u^{\ddagger}$ is only slightly smaller than β_I). Thus little additional unfolding occurs between I and the subsequent transition state. The decrease in solvent-accessible surface area between folding intermediates and main transition states is less than 10% for several other proteins (*10*).

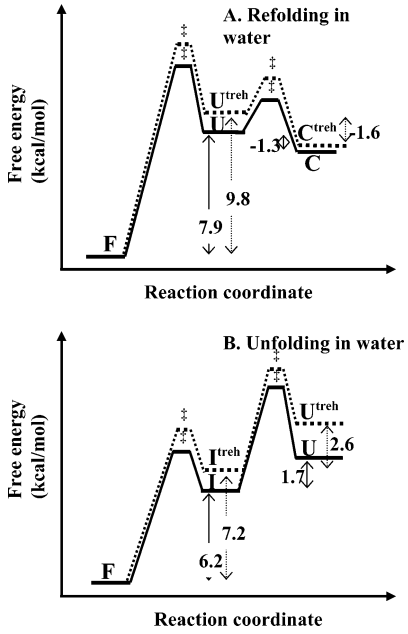

FIGURE 7: Free energy reaction profile for refolding (A) and unfolding (B) of cutinase in water at pH 4.5 in the absence (solid line) and presence of 0.75 M trehalose (dotted line). Values are the free energy change in kilocalories per mole. ΔG_{U-I} was calculated from the difference between ΔG_{U-F} from equilibrium data and ΔG_{I-F} from kinetic data.

The refolding kinetics reveal the presence of an intermediate C more compact than the transition state for folding (β_C is larger than $\beta_f^{\ddagger}$). The simplest interpretation is that a more compact intermediate accumulates, which is off the folding pathway. The presence of the intermediate becomes clearer in the presence of high trehalose concentrations. Above a certain trehalose concentration there is actually a decrease in the observable rate constant (Figure 6). As suggested in Scheme 2, this decrease is due to a shift in the equilibrium from U toward C and does not result from an increase in the free energy between the transition state and the ground state (Table 3). On the contrary, trehalose decreases the free energy between the transition state and the ground state for folding because k_f increases with trehalose concentration [$m^{\ddagger}{}_f^{trehalose}$ is positive (Table 3)]. The stabilization of an intermediate on-folding pathway by trehalose would result in a monotonic increase in the folding rate with trehalose concentration, because the more compact transition state will be more stabilized than the less compact ground state (the intermediate), from which folding occurs.

Equilibrium unfolding data show that trehalose increases the free energy change between the folded and unfolded cutinase (Table 1). This stabilizing effect of trehalose on more compact states (or destabilizing effect on less compact states) is also revealed by kinetic data (Table 2). The equilibrium constant between F and I (K_I^{water}) decreases and the equilibrium constant between U and C (K_C^{water}) increases with the increase on trehalose concentration. More compact states are favored (F versus I and C versus U) as shown in the free energy profile for folding and unfolding of cutinase in water (Figure 7). To draw a comprehensive free energy reaction profile, it was assumed that the free energy of the folded state was unaffected by trehalose. This is a simplification because we cannot conclude if trehalose stabilizes more compact or destabilizes less compact states; i.e., trehalose can stabilize more F than I and U or destabilize more U and I than F state. These free energy reaction profiles may underestimate the effect of trehalose since gravimetric concentrations of GdnHCl were used for the calculations and the thermodynamic activity of GdnHCl will increase in the presence of trehalose. The stabilization of more compact states was also observed for the kinetics of the three-state folding of ubiquitin in the presence of ammonium sulfate. Salt stabilizes both the partially and fully folded states relative to the unfolded state (*4*).

Timasheff and collaborators have proposed that RNase A stabilization by trehalose at room temperature is determined by an increase in preferential exclusion of trehalose upon unfolding (*18*). In other words, the immediate domain of the protein is poorer in trehalose than the bulk solvent for both the folded and unfolded state, but the effect is stronger for the unfolded state, and therefore this state is more destabilized than the folded state. This mechanism proposed to other osmolytes such as sorbitol (*19*), lactose and glucose (*20*), sucrose and sarcosine (*21*), and glycerol (*22, 23*) shows a predominant effect of the solute on the unfolded state. In molecular terms, the number of nonthermodynamically neutral contacts with loci on the protein surface decreases relative to those with water when the protein unfolds. The idea that species with smaller surface areas are favored over species with larger surface areas in the presence of sugars was already proposed. Bolen and colleagues (*21*) have proposed that decreased exposure of the backbone on folding is the major driving force for sucrose- and sarcosine-induced stabilization. For ferricytochrome *c* a new collapsed conformation (the A-state) became more stable than the acid-unfolded species in the presence of sugars (*24*). The increase of hydrophobic interactions induced by the water structure-maker solutes such as sugars and polyols (inducers of a cage structure in neighboring water) (*2*) may favor more compact states.

The results presented in this work show clearly that trehalose favors more compact states or disfavors less compact states. The paradigmatic example is the stabilization of C relative to the unfolded state. Despite its deceleration of folding, this compact intermediate with non-native contacts is stabilized by trehalose because of its reduced surface area. Since this collapse of the unfolded ensemble decreases the observable folding rate, it seems reasonable to suppose that the opening of the pathway from U to C is a "side effect" of the mechanism evolved through stabilization. It should be noted that the trehalose concentrations used were clearly in the physiological range, estimated to be up to 0.5 M in the cytoplasm (*25*). To counteract reduced folding rates under conditions where such a reduction can be deleterious to the cell (e.g., when intermediates accumulate which can aggregate), we have recently suggested that evolution has selected gatekeeping residues to destabilize compact intermediates (*3*).

ACKNOWLEDGMENT

We thank Prof. Sílvia B. M. Costa from Instituto Superior Técnico (IST) for support, namely, laboratory and fluorescence facilities, and Prof. Pombeiro from IST for stopped-flow facilities.

REFERENCES

1. Timasheff, S. N. (1995) Solvent stabilization of protein structure, in *Protein Stability and Folding: Theory and Practice* (Shirley, B. A., Ed.) pp 253−269, Humana Press, Totowa, NJ.
2. Back, J. F., Oakenfull, D., and Smith, M. B. (1979) Increased thermal stability of proteins in the presence of sugars and polyols, *Biochemistry 18*, 5191−5196.
3. Otzen, D. E., and Oliveberg, M. (1999) Salt-induced detour through compact regions of the protein folding landscape, *Proc. Natl. Acad. Sci. U.S.A. 96*, 11746−11751.
4. Khorasanizadeh, S., Peters, I. D., and Roder, H. (1996) Evidence for a three-state model of protein folding from kinetic analysis of ubiquitin variants with altered core residues, *Nat. Struct. Biol. 3*, 193−205.
5. Brown, A. D. (1990) Compatible solutes, in *Microbial water stress physiology. Principles and perspectives*, pp 241−275, John Wiley and Sons, New York.
6. Schiraldi, C., Di Lernia, I., and De Rosa, M. (2002) Trehalose production: exploiting novel approaches, *Trends Biotechnol. 20*, 420−425.
7. Singer, M. A., and Lindquist, S. (1998) Thermotolerance in *Saccharomyces cerevisiae*: The Yin and Yang of trehalose, *Trends Biotechnol. 16*, 460−468.
8. Koops, B. C., Verheij, H. M., Slotboom, A. J., and Egmond, M. R. (1999) Effect of chemical modification on the activity of lipases in organic solvents, *Enzyme Microb. Technol. 25*, 622−631.
9. Melo, E. P., Faria, T. Q., Martins, L. O., Gonçalves, A. M., and Cabral, J. M. S. (2001) Cutinase Unfolding and Stabilization by trehalose and mannosylglycerate, *Proteins 42*, 542−552.
10. Roder, H., and Colón, W. (1997) Kinetic role of early intermediates in protein folding, *Curr. Opin. Struct. Biol. 7*, 15−28.
11. Melo, E. P., Costa, S. M. B., and Cabral, J. M. S. (1996) Denaturation of a recombinant cutinase from *Fusarium solani* in AOT-*iso*-octane reverse micelles: a steady-state fluorescence study, *Photochem. Photobiol. 63*, 169−175.
12. Fersht, A. (1999) *Structure and Mechanism in Protein Science*, pp 540−572, W. H. Freeman, New York.
13. Silow, M., and Oliveberg, M. (1997) Transient aggregates in protein folding are easily mistaken for folding intermediates, *Proc. Natl. Acad. Sci. U.S.A. 94*, 6084−6086.
14. Brandts, J. F., Halvorson, H. R., and Brennan, M. (1975) Consideration of the possibility that the slow step in protein denaturation reaction is due to cis−trans isomerism of proline residues, *Biochemistry 14*, 4953−4963.
15. Silow, M., Oliveberg, M. (1997) High-Energy channelling in protein folding, *Biochemistry 36*, 7633−7637.
16. Otzen, D. E., Kristensen, O., Proctor, M., Oliveberg, M. (1999) Structural changes in the transition state of protein folding: Alternative interpretations of curved chevron plots, *Biochemistry 38*, 6499−6511.
17. Zaidi, F. N., Nath, U., and Udgaonkar, J. B. (1997) Multiple intermediates and transition states during protein unfolding, *Nat. Struct. Biol. 4*, 1016−1024.
18. Xie, G., and Timasheff, S. N. (1997) The thermodynamic mechanism of protein stabilization by trehalose, *Biophys. Chem. 64*, 25−43.
19. Xie, G., and Timasheff, S. N. (1997) Mechanism of the stabilization of ribonuclease A by sorbitol: Preferential hydration is greater for the denaturated than for the native protein, *Protein Sci. 6*, 211−221.
20. Arakawa, T., and Timasheff, S. N. (1982) Stabilization of protein structure by sugars, *Biochemistry 21*, 6536−6544.
21. Liu, Y., and Bolen, D. W. (1995) The peptide backbone plays a dominant role in protein stabilization by naturally occurring osmolytes, *Biochemistry 34*, 12884−12891.
22. Gekko, K., and Timasheff, S. N. (1981) Mechanism of protein stabilization by glycerol: Preferential hydration in glycerol-water mixtures, *Biochemistry 20*, 4667−4676.
23. Gekko, K., and Timasheff, S. N. (1981) Thermodynamic and kinetic examination of protein stabilization by glycerol, *Biochemistry 20*, 4677−4686.
24. Davis-Searles, P. R., Morar, A. S., Saunders, A. J., Frie, D. A., and Pielak, G. J. (1998) Sugar-induced molten-globule model, *Biochemistry 37*, 17048−17053.
25. Hottiger, T., De Virgilio, C., Hall, M. N., Boller, T., and Wiemken, A. (1994) The role of trehalose synthesis for the acquisition of thermotolerance in yeast. II. Physiological concentrations of trehalose increase the thermal stability of proteins in vitro, *Eur. J. Biochem. 219*, 187−193.

BI034267X